

Search for the standard model Higgs boson in tau final states

V.M. Abazov³⁷, B. Abbott⁷⁵, M. Abolins⁶⁵, B.S. Acharya³⁰, M. Adams⁵¹, T. Adams⁴⁹,
 E. Aguilo⁶, M. Ahsan⁵⁹, G.D. Alexeev³⁷, G. Alkhalaf⁴¹, A. Alton^{64,a}, G. Alverson⁶³,
 G.A. Alves², L.S. Ancu³⁶, T. Andeen⁵³, M.S. Anzels⁵³, M. Aoki⁵⁰, Y. Arnoud¹⁴, M. Arov⁶⁰,
 M. Arthaud¹⁸, A. Askew^{49,b}, B. Åsman⁴², O. Atramentov^{49,b}, C. Avila⁸, J. BackusMayes⁸²,
 F. Badaud¹³, L. Bagby⁵⁰, B. Baldin⁵⁰, D.V. Bandurin⁵⁹, S. Banerjee³⁰, E. Barberis⁶³,
 A.-F. Barfuss¹⁵, P. Bargassa⁸⁰, P. Baringer⁵⁸, J. Barreto², J.F. Bartlett⁵⁰, U. Bassler¹⁸,
 D. Bauer⁴⁴, S. Beale⁶, A. Bean⁵⁸, M. Begalli³, M. Begel⁷³, C. Belanger-Champagne⁴²,
 L. Bellantoni⁵⁰, A. Bellavance⁵⁰, J.A. Benitez⁶⁵, S.B. Beri²⁸, G. Bernardi¹⁷, R. Bernhard²³,
 I. Bertram⁴³, M. Besançon¹⁸, R. Beuselinck⁴⁴, V.A. Bezzubov⁴⁰, P.C. Bhat⁵⁰,
 V. Bhatnagar²⁸, G. Blazey⁵², S. Blessing⁴⁹, K. Bloom⁶⁷, A. Boehnlein⁵⁰, D. Boline⁶²,
 T.A. Bolton⁵⁹, E.E. Boos³⁹, G. Borissov⁴³, T. Bose⁶², A. Brandt⁷⁸, R. Brock⁶⁵,
 G. Brooijmans⁷⁰, A. Bross⁵⁰, D. Brown¹⁹, X.B. Bu⁷, D. Buchholz⁵³, M. Buehler⁸¹,
 V. Buescher²², V. Bunichev³⁹, S. Burdin^{43,c}, T.H. Burnett⁸², C.P. Buszello⁴⁴,
 P. Calfayan²⁶, B. Calpas¹⁵, S. Calvet¹⁶, J. Cammin⁷¹, M.A. Carrasco-Lizarraga³⁴,
 E. Carrera⁴⁹, W. Carvalho³, B.C.K. Casey⁵⁰, H. Castilla-Valdez³⁴, S. Chakrabarti⁷²,
 D. Chakraborty⁵², K.M. Chan⁵⁵, A. Chandra⁴⁸, E. Cheu⁴⁶, D.K. Cho⁶², S. Choi³³,
 B. Choudhary²⁹, T. Christoudias⁴⁴, S. Cihangir⁵⁰, D. Claes⁶⁷, J. Clutter⁵⁸, M. Cooke⁵⁰,
 W.E. Cooper⁵⁰, M. Corcoran⁸⁰, F. Couderc¹⁸, M.-C. Cousinou¹⁵, S. Crépe-Renaudin¹⁴,
 V. Cuplov⁵⁹, D. Cutts⁷⁷, M. Ćwiok³¹, A. Das⁴⁶, G. Davies⁴⁴, K. De⁷⁸, S.J. de Jong³⁶,
 E. De La Cruz-Burelo³⁴, K. DeVaughan⁶⁷, F. Déliot¹⁸, M. Demarteau⁵⁰, R. Demina⁷¹,
 D. Denisov⁵⁰, S.P. Denisov⁴⁰, S. Desai⁵⁰, H.T. Diehl⁵⁰, M. Diesburg⁵⁰, A. Dominguez⁶⁷,
 T. Dorland⁸², A. Dubey²⁹, L.V. Dudko³⁹, L. Duflo¹⁶, D. Duggan⁴⁹, A. Duperrin¹⁵,
 S. Dutt²⁸, A. Dyshkant⁵², M. Eads⁶⁷, D. Edmunds⁶⁵, J. Ellison⁴⁸, V.D. Elvira⁵⁰, Y. Enari⁷⁷,
 S. Eno⁶¹, P. Ermolov^{39,‡}, M. Escalier¹⁵, H. Evans⁵⁴, A. Evdokimov⁷³, V.N. Evdokimov⁴⁰,
 G. Facini⁶³, A.V. Ferapontov⁵⁹, T. Ferbel^{61,71}, F. Fiedler²⁵, F. Filthaut³⁶, W. Fisher⁵⁰,
 H.E. Fisk⁵⁰, M. Fortner⁵², H. Fox⁴³, S. Fu⁵⁰, S. Fuess⁵⁰, T. Gadfort⁷⁰, C.F. Galea³⁶,
 A. Garcia-Bellido⁷¹, V. Gavrilov³⁸, P. Gay¹³, W. Geist¹⁹, W. Geng^{15,65}, C.E. Gerber⁵¹,

Y. Gershtein^{49,b}, D. Gillberg⁶, G. Ginther^{50,71}, B. Gómez⁸, A. Goussiou⁸², P.D. Grannis⁷²,
 S. Greder¹⁹, H. Greenlee⁵⁰, Z.D. Greenwood⁶⁰, E.M. Gregores⁴, G. Grenier²⁰, Ph. Gris¹³,
 J.-F. Grivaz¹⁶, A. Grohsjean²⁶, S. Grünendahl⁵⁰, M.W. Grünewald³¹, F. Guo⁷², J. Guo⁷²,
 G. Gutierrez⁵⁰, P. Gutierrez⁷⁵, A. Haas⁷⁰, N.J. Hadley⁶¹, P. Haefner²⁶, S. Hagopian⁴⁹,
 J. Haley⁶⁸, I. Hall⁶⁵, R.E. Hall⁴⁷, L. Han⁷, K. Harder⁴⁵, A. Harel⁷¹, J.M. Hauptman⁵⁷,
 J. Hays⁴⁴, T. Hebbeker²¹, D. Hedin⁵², J.G. Hegeman³⁵, A.P. Heinson⁴⁸, U. Heintz⁶²,
 C. Hensel²⁴, I. Heredia-De La Cruz³⁴, K. Herner⁶⁴, G. Hesketh⁶³, M.D. Hildreth⁵⁵,
 R. Hirosky⁸¹, T. Hoang⁴⁹, J.D. Hobbs⁷², B. Hoeneisen¹², M. Hohlfeld²², S. Hossain⁷⁵,
 P. Houben³⁵, Y. Hu⁷², Z. Hubacek¹⁰, N. Huske¹⁷, V. Hynek¹⁰, I. Iashvili⁶⁹, R. Illingworth⁵⁰,
 A.S. Ito⁵⁰, S. Jabeen⁶², M. Jaffré¹⁶, S. Jain⁷⁵, K. Jakobs²³, D. Jamin¹⁵, C. Jarvis⁶¹,
 R. Jesik⁴⁴, K. Johns⁴⁶, C. Johnson⁷⁰, M. Johnson⁵⁰, D. Johnston⁶⁷, A. Jonckheere⁵⁰,
 P. Jonsson⁴⁴, A. Juste⁵⁰, E. Kajfasz¹⁵, D. Karmanov³⁹, P.A. Kasper⁵⁰, I. Katsanos⁶⁷,
 V. Kaushik⁷⁸, R. Kehoe⁷⁹, S. Kermiche¹⁵, N. Khalatyan⁵⁰, A. Khanov⁷⁶, A. Kharchilava⁶⁹,
 Y.N. Kharzheev³⁷, D. Khatidze⁷⁰, T.J. Kim³², M.H. Kirby⁵³, M. Kirsch²¹, B. Klima⁵⁰,
 J.M. Kohli²⁸, J.-P. Konrath²³, A.V. Kozelov⁴⁰, J. Kraus⁶⁵, T. Kuhl²⁵, A. Kumar⁶⁹,
 A. Kupco¹¹, T. Kurča²⁰, V.A. Kuzmin³⁹, J. Kvita⁹, F. Lacroix¹³, D. Lam⁵⁵,
 S. Lammers⁵⁴, G. Landsberg⁷⁷, P. Lebrun²⁰, W.M. Lee⁵⁰, A. Leflat³⁹, J. Lellouch¹⁷,
 J. Li^{78,‡}, L. Li⁴⁸, Q.Z. Li⁵⁰, S.M. Lietti⁵, J.K. Lim³², D. Lincoln⁵⁰, J. Linnemann⁶⁵,
 V.V. Lipaev⁴⁰, R. Lipton⁵⁰, Y. Liu⁷, Z. Liu⁶, A. Lobodenko⁴¹, M. Lokajicek¹¹,
 P. Love⁴³, H.J. Lubatti⁸², R. Luna-Garcia^{34,d}, A.L. Lyon⁵⁰, A.K.A. Maciel²,
 D. Mackin⁸⁰, P. Mättig²⁷, A. Magerkurth⁶⁴, P.K. Mal⁸², H.B. Malbouisson³, S. Malik⁶⁷,
 V.L. Malyshev³⁷, Y. Maravin⁵⁹, B. Martin¹⁴, R. McCarthy⁷², C.L. McGivern⁵⁸,
 M.M. Meijer³⁶, A. Melnitchouk⁶⁶, L. Mendoza⁸, D. Menezes⁵², P.G. Mercadante⁵,
 M. Merkin³⁹, K.W. Merritt⁵⁰, A. Meyer²¹, J. Meyer²⁴, J. Mitrevski⁷⁰, R.K. Mommsen⁴⁵,
 N.K. Mondal³⁰, R.W. Moore⁶, T. Moulik⁵⁸, G.S. Muanza¹⁵, M. Mulhearn⁷⁰, O. Mundal²²,
 L. Mundim³, E. Nagy¹⁵, M. Naimuddin⁵⁰, M. Narain⁷⁷, H.A. Neal⁶⁴, J.P. Negret⁸,
 P. Neustroev⁴¹, H. Nilsen²³, H. Nogima³, S.F. Novaes⁵, T. Nunnemann²⁶, G. Obrant⁴¹,
 C. Ochando¹⁶, D. Onoprienko⁵⁹, J. Orduna³⁴, N. Oshima⁵⁰, N. Osman⁴⁴, J. Osta⁵⁵,
 R. Otec¹⁰, G.J. Otero y Garzón¹, M. Owen⁴⁵, M. Padilla⁴⁸, P. Padley⁸⁰, M. Pangilinan⁷⁷,
 N. Parashar⁵⁶, S.-J. Park²⁴, S.K. Park³², J. Parsons⁷⁰, R. Partridge⁷⁷, N. Parua⁵⁴,

A. Patwa⁷³, G. Pawloski⁸⁰, B. Penning²³, M. Perfilov³⁹, K. Peters⁴⁵, Y. Peters⁴⁵,
 P. Pétroff¹⁶, R. Piegaia¹, J. Piper⁶⁵, M.-A. Pleier²², P.L.M. Podesta-Lerma^{34,e},
 V.M. Podstavkov⁵⁰, Y. Pogorelov⁵⁵, M.-E. Pol², P. Polozov³⁸, A.V. Popov⁴⁰, C. Potter⁶,
 W.L. Prado da Silva³, S. Protopopescu⁷³, J. Qian⁶⁴, A. Quadt²⁴, B. Quinn⁶⁶,
 A. Rakitine⁴³, M.S. Rangel¹⁶, K. Ranjan²⁹, P.N. Ratoff⁴³, P. Renkel⁷⁹, P. Rich⁴⁵,
 M. Rijssenbeek⁷², I. Ripp-Baudot¹⁹, F. Rizatdinova⁷⁶, S. Robinson⁴⁴, R.F. Rodrigues³,
 M. Rominsky⁷⁵, C. Royon¹⁸, P. Rubinov⁵⁰, R. Ruchti⁵⁵, G. Safronov³⁸, G. Sajot¹⁴,
 A. Sánchez-Hernández³⁴, M.P. Sanders¹⁷, B. Sanghi⁵⁰, G. Savage⁵⁰, L. Sawyer⁶⁰,
 T. Scanlon⁴⁴, D. Schaile²⁶, R.D. Schamberger⁷², Y. Scheglov⁴¹, H. Schellman⁵³,
 T. Schliephake²⁷, S. Schlobohm⁸², C. Schwanenberger⁴⁵, R. Schwienhorst⁶⁵, J. Sekaric⁴⁹,
 H. Severini⁷⁵, E. Shabalina²⁴, M. Shamim⁵⁹, V. Shary¹⁸, A.A. Shchukin⁴⁰, R.K. Shivpuri²⁹,
 V. Siccaldi¹⁹, V. Simak¹⁰, V. Sirotenko⁵⁰, P. Skubic⁷⁵, P. Slattery⁷¹, D. Smirnov⁵⁵,
 G.R. Snow⁶⁷, J. Snow⁷⁴, S. Snyder⁷³, S. Söldner-Rembold⁴⁵, L. Sonnenschein²¹,
 A. Sopczak⁴³, M. Sosebee⁷⁸, K. Soustruznik⁹, B. Spurlock⁷⁸, J. Stark¹⁴, V. Stolin³⁸,
 D.A. Stoyanova⁴⁰, J. Strandberg⁶⁴, S. Strandberg⁴², M.A. Strang⁶⁹, E. Strauss⁷²,
 M. Strauss⁷⁵, R. Ströhmer²⁶, D. Strom⁵³, L. Stutte⁵⁰, S. Sumowidagdo⁴⁹, P. Svoisky³⁶,
 M. Takahashi⁴⁵, A. Tanasijczuk¹, W. Taylor⁶, B. Tiller²⁶, F. Tissandier¹³, M. Titov¹⁸,
 V.V. Tokmenin³⁷, I. Torchiani²³, D. Tsybychev⁷², B. Tuchming¹⁸, C. Tully⁶⁸, P.M. Tuts⁷⁰,
 R. Unalan⁶⁵, L. Uvarov⁴¹, S. Uvarov⁴¹, S. Uzunyan⁵², B. Vachon⁶, P.J. van den Berg³⁵,
 R. Van Kooten⁵⁴, W.M. van Leeuwen³⁵, N. Varelas⁵¹, E.W. Varnes⁴⁶, I.A. Vasilyev⁴⁰,
 P. Verdier²⁰, L.S. Vertogradov³⁷, M. Verzocchi⁵⁰, D. Vilanova¹⁸, P. Vint⁴⁴, P. Vokac¹⁰,
 M. Voutilainen^{67,f}, R. Wagner⁶⁸, H.D. Wahl⁴⁹, M.H.L.S. Wang⁷¹, J. Warchol⁵⁵, G. Watts⁸²,
 M. Wayne⁵⁵, G. Weber²⁵, M. Weber^{50,g}, L. Welty-Rieger⁵⁴, A. Wenger^{23,h}, M. Wetstein⁶¹,
 A. White⁷⁸, D. Wicke²⁵, M.R.J. Williams⁴³, G.W. Wilson⁵⁸, S.J. Wimpenny⁴⁸,
 M. Wobisch⁶⁰, D.R. Wood⁶³, T.R. Wyatt⁴⁵, Y. Xie⁷⁷, C. Xu⁶⁴, S. Yacoob⁵³, R. Yamada⁵⁰,
 W.-C. Yang⁴⁵, T. Yasuda⁵⁰, Y.A. Yatsunenko³⁷, Z. Ye⁵⁰, H. Yin⁷, K. Yip⁷³, H.D. Yoo⁷⁷,
 S.W. Youn⁵³, J. Yu⁷⁸, C. Zeitnitz²⁷, S. Zelitch⁸¹, T. Zhao⁸², B. Zhou⁶⁴, J. Zhu⁷²,
 M. Zielinski⁷¹, D. Zieminska⁵⁴, L. Zivkovic⁷⁰, V. Zutshi⁵², and E.G. Zverev³⁹

(The DØ Collaboration)

¹ *Universidad de Buenos Aires, Buenos Aires, Argentina*

- ²*LAFEX, Centro Brasileiro de Pesquisas Físicas, Rio de Janeiro, Brazil*
- ³*Universidade do Estado do Rio de Janeiro, Rio de Janeiro, Brazil*
- ⁴*Universidade Federal do ABC, Santo André, Brazil*
- ⁵*Instituto de Física Teórica, Universidade Estadual Paulista, São Paulo, Brazil*
- ⁶*University of Alberta, Edmonton, Alberta, Canada; Simon Fraser University, Burnaby, British Columbia, Canada; York University, Toronto, Ontario, Canada and McGill University, Montreal, Quebec, Canada*
- ⁷*University of Science and Technology of China, Hefei, People's Republic of China*
- ⁸*Universidad de los Andes, Bogotá, Colombia*
- ⁹*Center for Particle Physics, Charles University, Faculty of Mathematics and Physics, Prague, Czech Republic*
- ¹⁰*Czech Technical University in Prague, Prague, Czech Republic*
- ¹¹*Center for Particle Physics, Institute of Physics, Academy of Sciences of the Czech Republic, Prague, Czech Republic*
- ¹²*Universidad San Francisco de Quito, Quito, Ecuador*
- ¹³*LPC, Université Blaise Pascal, CNRS/IN2P3, Clermont, France*
- ¹⁴*LPSC, Université Joseph Fourier Grenoble 1, CNRS/IN2P3, Institut National Polytechnique de Grenoble, Grenoble, France*
- ¹⁵*CPPM, Aix-Marseille Université, CNRS/IN2P3, Marseille, France*
- ¹⁶*LAL, Université Paris-Sud, IN2P3/CNRS, Orsay, France*
- ¹⁷*LPNHE, IN2P3/CNRS, Universités Paris VI and VII, Paris, France*
- ¹⁸*CEA, Irfu, SPP, Saclay, France*
- ¹⁹*IPHC, Université de Strasbourg, CNRS/IN2P3, Strasbourg, France*
- ²⁰*IPNL, Université Lyon 1, CNRS/IN2P3, Villeurbanne, France and Université de Lyon, Lyon, France*
- ²¹*III. Physikalisches Institut A, RWTH Aachen University, Aachen, Germany*
- ²²*Physikalisches Institut, Universität Bonn, Bonn, Germany*
- ²³*Physikalisches Institut, Universität Freiburg, Freiburg, Germany*
- ²⁴*II. Physikalisches Institut, Georg-August-Universität G Göttingen, Germany*

- ²⁵*Institut für Physik, Universität Mainz, Mainz, Germany*
- ²⁶*Ludwig-Maximilians-Universität München, München, Germany*
- ²⁷*Fachbereich Physik, University of Wuppertal, Wuppertal, Germany*
- ²⁸*Panjab University, Chandigarh, India*
- ²⁹*Delhi University, Delhi, India*
- ³⁰*Tata Institute of Fundamental Research, Mumbai, India*
- ³¹*University College Dublin, Dublin, Ireland*
- ³²*Korea Detector Laboratory, Korea University, Seoul, Korea*
- ³³*SungKyunKwan University, Suwon, Korea*
- ³⁴*CINVESTAV, Mexico City, Mexico*
- ³⁵*FOM-Institute NIKHEF and University of
Amsterdam/NIKHEF, Amsterdam, The Netherlands*
- ³⁶*Radboud University Nijmegen/NIKHEF, Nijmegen, The Netherlands*
- ³⁷*Joint Institute for Nuclear Research, Dubna, Russia*
- ³⁸*Institute for Theoretical and Experimental Physics, Moscow, Russia*
- ³⁹*Moscow State University, Moscow, Russia*
- ⁴⁰*Institute for High Energy Physics, Protvino, Russia*
- ⁴¹*Petersburg Nuclear Physics Institute, St. Petersburg, Russia*
- ⁴²*Stockholm University, Stockholm, Sweden,
and Uppsala University, Uppsala, Sweden*
- ⁴³*Lancaster University, Lancaster, United Kingdom*
- ⁴⁴*Imperial College, London, United Kingdom*
- ⁴⁵*University of Manchester, Manchester, United Kingdom*
- ⁴⁶*University of Arizona, Tucson, Arizona 85721, USA*
- ⁴⁷*California State University, Fresno, California 93740, USA*
- ⁴⁸*University of California, Riverside, California 92521, USA*
- ⁴⁹*Florida State University, Tallahassee, Florida 32306, USA*
- ⁵⁰*Fermi National Accelerator Laboratory, Batavia, Illinois 60510, USA*
- ⁵¹*University of Illinois at Chicago, Chicago, Illinois 60607, USA*
- ⁵²*Northern Illinois University, DeKalb, Illinois 60115, USA*

- ⁵³*Northwestern University, Evanston, Illinois 60208, USA*
- ⁵⁴*Indiana University, Bloomington, Indiana 47405, USA*
- ⁵⁵*University of Notre Dame, Notre Dame, Indiana 46556, USA*
- ⁵⁶*Purdue University Calumet, Hammond, Indiana 46323, USA*
- ⁵⁷*Iowa State University, Ames, Iowa 50011, USA*
- ⁵⁸*University of Kansas, Lawrence, Kansas 66045, USA*
- ⁵⁹*Kansas State University, Manhattan, Kansas 66506, USA*
- ⁶⁰*Louisiana Tech University, Ruston, Louisiana 71272, USA*
- ⁶¹*University of Maryland, College Park, Maryland 20742, USA*
- ⁶²*Boston University, Boston, Massachusetts 02215, USA*
- ⁶³*Northeastern University, Boston, Massachusetts 02115, USA*
- ⁶⁴*University of Michigan, Ann Arbor, Michigan 48109, USA*
- ⁶⁵*Michigan State University, East Lansing, Michigan 48824, USA*
- ⁶⁶*University of Mississippi, University, Mississippi 38677, USA*
- ⁶⁷*University of Nebraska, Lincoln, Nebraska 68588, USA*
- ⁶⁸*Princeton University, Princeton, New Jersey 08544, USA*
- ⁶⁹*State University of New York, Buffalo, New York 14260, USA*
- ⁷⁰*Columbia University, New York, New York 10027, USA*
- ⁷¹*University of Rochester, Rochester, New York 14627, USA*
- ⁷²*State University of New York, Stony Brook, New York 11794, USA*
- ⁷³*Brookhaven National Laboratory, Upton, New York 11973, USA*
- ⁷⁴*Langston University, Langston, Oklahoma 73050, USA*
- ⁷⁵*University of Oklahoma, Norman, Oklahoma 73019, USA*
- ⁷⁶*Oklahoma State University, Stillwater, Oklahoma 74078, USA*
- ⁷⁷*Brown University, Providence, Rhode Island 02912, USA*
- ⁷⁸*University of Texas, Arlington, Texas 76019, USA*
- ⁷⁹*Southern Methodist University, Dallas, Texas 75275, USA*
- ⁸⁰*Rice University, Houston, Texas 77005, USA*
- ⁸¹*University of Virginia, Charlottesville, Virginia 22901, USA and*
- ⁸²*University of Washington, Seattle, Washington 98195, USA*

(Dated: March 27, 2009)

Abstract

We present a search for the standard model Higgs boson using hadronically decaying tau leptons, in 1 fb^{-1} of data collected with the D0 detector at the Fermilab Tevatron $p\bar{p}$ collider. We select two final states: τ^\pm plus missing transverse energy and b jets, and $\tau^+\tau^-$ plus jets. These final states are sensitive to a combination of associated W/Z boson plus Higgs boson, vector boson fusion and gluon-gluon fusion production processes. The observed ratio of the combined limit on the Higgs production cross section at the 95% C.L. to the standard model expectation is 29 for a Higgs boson mass of 115 GeV.

PACS numbers: 13.85Qk, 13.85.Rm, 14.80Bn

A standard model (SM) Higgs boson with a mass in the range 105 – 145 GeV is expected to be produced in $p\bar{p}$ collisions at a center-of-mass energy of 2 TeV with cross sections of $\mathcal{O}(100 \text{ fb})$ for associated VH production ($V = W$ or Z) and vector boson fusion (VBF), $q\bar{q} \rightarrow VVq'\bar{q}'' \rightarrow q'\bar{q}''H$, and of $\mathcal{O}(1 \text{ pb})$ for gluon-gluon fusion (GGF) [1]. Previous searches for the SM Higgs boson at the Fermilab Tevatron collider [2] have sought the VH processes with W/Z decays to leptons other than taus and $H \rightarrow b\bar{b}$, and the gluon fusion process with $H \rightarrow VV^*$ with $V(V^*) \rightarrow ee$ or $\mu\mu$. Thus far, there have been no published searches in the case that either the V or H decays to τ leptons. Given the small Higgs boson production cross sections, it is advantageous to use all possible decay modes to increase the search sensitivity. Here, we present a search designed for either of the two final states: $\tau^\pm\nu + b\bar{b}$ jets (denoted “ $\tau\nu$ ”) or $\tau^+\tau^- +$ jets (denoted “ $\tau\tau$ ”). The analysis is based on 0.94 fb^{-1} ($\tau\nu$) and 1.02 fb^{-1} ($\tau\tau$) of data collected by the D0 experiment [3] at the Fermilab Tevatron collider.

The $\tau\nu$ analysis targets WH production with $W \rightarrow \tau\nu$ and ZH production where $Z \rightarrow \tau\tau$ but one τ is not identified, both with $H \rightarrow b\bar{b}$. The triggers used for selecting events require jets of high transverse energy, E_T , and large missing transverse energy, \cancel{E}_T . The offline selection of events requires at least one tau candidate decaying to hadrons, at least two jets identified as candidate b quark jets (b tagged) with transverse momentum $p_T > 15 \text{ GeV}$, and \cancel{E}_T , corrected for the presence of muons and taus, greater than 30 GeV. We reject events containing an electron with $p_T > 15 \text{ GeV}$ or a muon with $p_T > 8 \text{ GeV}$ to maintain independence from the $\tau\tau$ analysis and other SM Higgs boson searches [2].

The $\tau\tau$ analysis targets VH production with $Z \rightarrow \tau^+\tau^-$ and $H \rightarrow b\bar{b}$ (denoted “HZ”), $V \rightarrow q\bar{q}$ and $H \rightarrow \tau^+\tau^-$ (“WH” and “ZH”), VBF with $H \rightarrow \tau^+\tau^-$, and GGF with $H \rightarrow \tau^+\tau^-$ and at least two associated jets. We identify one of the taus through its decay to $\mu\nu\tau\bar{\nu}\mu$ and the other in a hadronic decay mode. The events satisfy a combination of single muon and muon plus jets trigger conditions. Offline, events are selected [4] by requiring exactly one muon with $p_T > 12 \text{ GeV}$, pseudorapidity $|\eta| < 2.0$, and isolated from other tracks and calorimeter activity in a cone surrounding the muon track candidate. We also require a hadronic tau candidate and at least two jets. The τ and μ are required to be of opposite charge for the primary event sample. Events containing an electron with $p_T > 12 \text{ GeV}$ are rejected.

We identify three types of hadronic taus, motivated by the decays (1) $\tau^\pm \rightarrow \pi^\pm\nu$, (2) $\tau^\pm \rightarrow \pi^\pm\pi^0\nu$, and (3) $\tau^\pm \rightarrow \pi^\pm\pi^\pm\pi^\mp(\pi^0)\nu$. The identifications [5] are based on the number

of associated tracks and activity in the electromagnetic (EM) portion of the calorimeter, both within a cone $\mathcal{R} = \sqrt{(\Delta\eta)^2 + (\Delta\phi)^2} < 0.5$, where ϕ is the azimuthal angle. The requirements for the $\tau\nu$ ($\tau\tau$) analysis are: for type 1, a single track with $p_T^{\text{trk}} > 12$ (15) GeV and no nearby EM energy cluster; for type 2, a single track with $p_T^{\text{trk}} > 10$ (15) GeV with an associated EM cluster, and for type 3, at least one track with $p_T^{\text{trk}} > 7$ GeV and $\Sigma p_T^{\text{trk}} > 20$ GeV and an associated EM cluster. In addition to hadronic tau decays, type 2 taus also contain $\tau \rightarrow e$ decays. Due to the larger multijet background, type 3 taus are not used in the $\tau\nu$ analysis. For the $\tau\tau$ channel only those two-track type 3 candidates with both tracks of the same charge sign are retained to give unambiguous tau charge determination. A neural network (NN) [5] is formed for each tau type using input variables such as isolation and the transverse and longitudinal shower profiles of the calorimeter energy depositions associated with the tau candidate. Tau preselection is based on the requirement that the output NN value, NN_τ , exceeds 0.3 thus favoring the tau hypothesis. The tau transverse momentum p_T^τ is constructed from the transverse energy observed in the calorimeter, E_T^τ , with type-dependent corrections based on the tracking information. For the three types we require p_T^τ to be greater than 12 (15), 10 (15), or (20) GeV for the $\tau\nu$ ($\tau\tau$) analyses. The $\tau\nu$ analysis subdivides the type 2 taus according to whether the energy deposit is electron-like or hadron-like and the two subsamples are treated separately in assessing the multijet background. For type 2 candidates in the $\tau\tau$ analysis, we require $0.7 < p_T^{\text{trk}}/E_T^\tau < 2$ to remove backgrounds in regions with poor EM calorimetry or due to cosmic rays.

Jets are reconstructed with a cone of radius 0.5 in rapidity-azimuth space [6]. Their energies are corrected to the particle level to account for detector effects and missing energy due to semileptonic decays of jet fragmentation products. We preselect jets with $p_T > 15$ GeV, $|\eta| < 2.5$, and separated by $\mathcal{R} > 0.5$ from τ and μ candidates.

Backgrounds other than those from multijet (MJ) production are simulated using Monte Carlo (MC). We use ALPGEN [7] for $t\bar{t}$ and V +jets production; PYTHIA [8] for WW , WZ and ZZ (diboson) production; and COMPHEP [9] for single top quark production. The ALPGEN events are passed through PYTHIA for parton showering and hadronization. The Higgs boson signal processes are generated using PYTHIA and the CTEQ6L1 [10] leading order parton distribution functions (PDF) for $M_H = 105 - 145$ GeV in 10 GeV steps. We normalize the cross sections to the highest available order calculations for the signal [11] and background [12]. Higgs decays are simulated using HDECAY [13] and for tau decays

using TAUOLA [14]. All MC events are passed through the standard D0 detector simulation, digitization, and reconstruction programs.

Backgrounds due to MJ production, with spurious \cancel{E}_T or misidentified taus are estimated from data samples. For the $\tau\nu$ analysis, an enriched multijet sample is formed by selecting taus with $0.3 < NN_\tau < 0.7$. The contributions from those background processes generated by MC are then subtracted to give the $BG_{\tau\nu}$ multijet background sample which has negligible Higgs boson signal and provides the shapes of the multijet distributions in the kinematic variables. The normalization is given by the ratio of the number of events in the signal region, $NN_\tau > 0.9$, after subtracting MC backgrounds, to the number of events in the $BG_{\tau\nu}$ sample.

For the MJ background in the $\tau\tau$ analysis, we prepare a multijet background data sample ($BG_{\tau\tau}$), orthogonal to the signal sample ($SG_{\tau\tau}$) defined by the μ , τ , and jet preselection cuts above, by reversing both track and calorimeter isolation requirements for the muon and by requiring $NN_\tau < 0.8$. For both $BG_{\tau\tau}$ and $SG_{\tau\tau}$ samples, the MC backgrounds are subtracted, and the same sign (SS) or opposite sign (OS) $\mu - \tau$ charge combinations subsets are formed. The $BG_{\tau\tau}$ sample provides the shape of the multijet background, with the normalization obtained by multiplying the number of SS $SG_{\tau\tau}$ events by the ratio of OS to SS events in the $BG_{\tau\tau}$ sample. These ratios are determined separately for each tau type, and are observed to be close to one and independent of p_T^μ and p_T^τ .

The event sample for the $\tau\nu$ analysis is obtained with additional requirements after the object selections described above: (a) at least two jets with $p_T > 20$ GeV and ≤ 3 jets with $p_T > 15$ GeV; (b) the angle $\Delta\phi(\cancel{E}_T, \cancel{T}_T) < \pi/2$, where \cancel{T}_T is the negative of the transverse component of the net momentum of all tracks in the event [15]; (c) $H_T < 200$ GeV, where H_T is the scalar sum of the p_T of all jets; (d) for hadron-like type 2 taus, the transverse mass, formed from the τ and \cancel{E}_T , less than 80 GeV; (e) dijet invariant mass in the range $50 < M_{jj} < 200$ GeV; and (f) the requirement $\Delta\phi(\tau, \cancel{E}_T) < 0.02(\pi - 2)(\cancel{E}_T - 30) + 2$ (\cancel{E}_T in GeV) to reduce contamination due to poorly reconstructed multijet events in which a jet misidentified as a tau is nearly collinear with \cancel{E}_T . To further improve the signal (S) over background (B) separation, we require two jets to be tagged with a NN that discriminates b quark jets and jets from light partons [16]. Figure 1(a,b) shows the M_{jj} distribution before and after b tagging and the event yields are summarized in Table I.

Most of the signal processes sought in the $\tau\tau$ analysis contain light quark jets, so we do

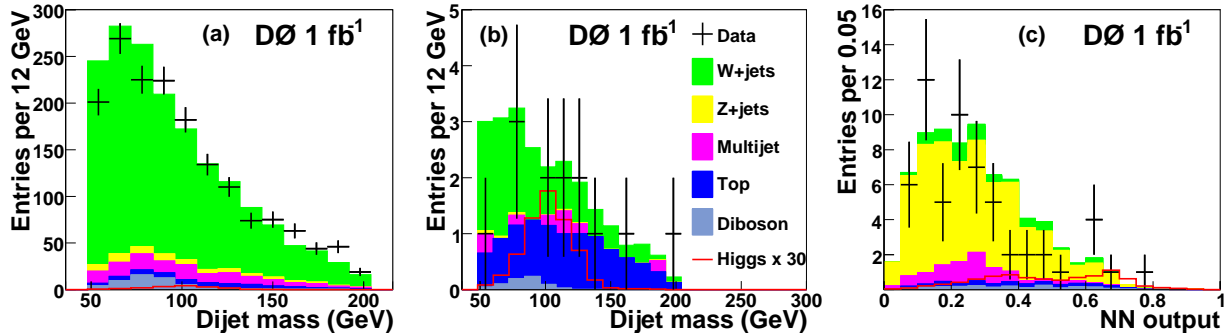


FIG. 1: The dijet mass distribution for all tau types for the $\tau\nu$ analysis (a) before b -tagging, and (b) after the final selection; (c) the combined $NN_{Z_{\text{jets}}}$ variable for the low Higgs mass $\tau\tau$ analysis. The signal is shown (multiplied by 30) for $M_H = 115$ GeV. (color online)

not employ b tagging. We require 2 jets with $p_T > 20$ GeV. To further separate signals from backgrounds, we train a dedicated NN for the signal processes (HZ, WH, ZH, VBF) and for each of the main background types ($W + \text{jets}$, $Z + \text{jets}$, $t\bar{t}$ and MJ). After requiring two jets, the MC GGF samples are small, making NN training unreliable. Since the GGF and VBF processes both involve non-resonant dijet systems, we incorporate the GGF events with the VBF sample when constructing the final limit analysis. The NNs are separately trained for low mass (105, 115 and 125 GeV) and high mass (135, 145 GeV) Higgs bosons, giving 32 NNs in all. Twenty well-modeled input variables are considered for each of the NNs. They include transverse or invariant masses of combinations of jets and leptons, \cancel{E}_T , angular correlations, and overall event distributions such as H_T and aplanarity[17]. For each signal-background pair, a choice of six or seven variables is made using the criterion that each added variable must give significant improvement in S/\sqrt{B} . The same variable choices are made for all Higgs boson masses. All NN input and output variables show good agreement between data and background prediction, and typically provide good discrimination between the signal and background under consideration. The $t\bar{t}$, $W + \text{jets}$ and MJ NNs give good separation of signal and background, whereas the $Z + \text{jets}$ NN signal and background distributions are not so well differentiated. Thus we define the variables NN_{bg} as the largest NN output variable among the various signals, for each background source, $\text{bg} = t\bar{t}$, $W + \text{jets}$, and MJ. We require $NN_{\text{bg}} > 0.4$, based on an optimization of the expected Higgs boson cross section limits. After this selection, the NN outputs trained against the $Z + \text{jets}$ background for all

TABLE I: Numbers of events at the preselection level and after the final selection (b tagging for $\tau\nu$ and NN_{bg} cut for $\tau\tau$) for all τ types combined, for data, estimated backgrounds and signal at $M_H = 115$ GeV. The V +jets background is given for light parton (“u,d,s,g” = “lp”) and heavy flavor (“b,c” = “hf”) jets separately. The uncertainties shown are statistical only. For the $\tau\nu$ ($\tau\tau$) analysis the combined statistical and systematic uncertainties on the sum of backgrounds in the final selections are 5.3 (14.8) events.

Source	$\tau\nu$ analysis		$\tau\tau$ analysis	
	Preselection	Final	Preselection	Final
$W + \text{lp}$	1124 ± 18	0.5 ± 0.0	37.7 ± 2.1	5.1 ± 0.3
$W + \text{hf}$	308.2 ± 4.8	10.9 ± 0.3	8.2 ± 0.5	0.9 ± 0.1
$Z + \text{lp}$	49.1 ± 1.5	< 0.2	78.4 ± 0.9	43.8 ± 0.6
$Z + \text{hf}$	7.8 ± 0.5	0.4 ± 0.0	15.7 ± 1.0	10.1 ± 0.7
$t\bar{t}$	46.7 ± 0.4	9.5 ± 0.1	30.8 ± 0.3	2.8 ± 0.0
Diboson	54.9 ± 1.1	0.7 ± 0.0	6.1 ± 0.5	2.1 ± 0.2
Multijet	122.6 ± 11.2	1.3 ± 0.1	57.2 ± 8.1	6.5 ± 2.8
Sum	1714 ± 22	23.3 ± 0.4	234 ± 9	71.2 ± 3.0
Data	1666	13	220	58
HZ			0.038	0.029
WH	0.543	0.201	0.145	0.106
ZH	0.023	0.015	0.094	0.069
VBF			0.071	0.059
GGF			0.041	0.030
Sum	0.566	0.216	0.389	0.293

signals are combined by taking their weighted average, NN_{Zjets} , over the four signal processes (HZ, WH, ZH, VBF), with weights equal to the relative expected yield for each signal. The NN_{Zjets} distribution for the final sample is shown in Fig. 1(c), now including the GGF signal events. The signal and background event yields are given in Table I.

Some systematic uncertainties induce a shape dependence on the final limit setting variable. For the $\tau\nu$ analysis, such shape dependence is found for the jet energy scale, jet energy

resolution, and the b -tagging efficiencies. Alternate shapes are determined by changing the relevant parameter by ± 1 standard deviation from the nominal value and are provided to the limit setting program. For the $\tau\tau$ analysis, only the multijet background is found to give an appreciable shape change. It is determined by varying the method for selecting MJ events, reversing either the muon or the tau requirements, but not both, relative to the standard choice. The remaining ‘flat’ systematic uncertainties do not affect the final variable distribution shape. Such flat uncertainties for the $\tau\nu$ ($\tau\tau$) analysis are, unless otherwise noted, fully correlated for different backgrounds and analysis channels, and include (a) integrated luminosity, 6.1% (6.1%) [18]; (b) trigger efficiency, 5.5% (3%) (uncorrelated $\tau\nu$ and $\tau\tau$); (c) muon identification, (4.5%); (d) tau identification, 5.0–6.0% (5.0%); (e) tau track efficiency, 3.0% (3.0%); (f) tau energy scale, 2.3–2.7% (3.5%); (g) jet identification and reconstruction, 1.7–4.9% (2%); (h) jet energy resolution, (4.5%); (i) jet energy scale (7.5%) [19]; (j) MC background cross sections, 6–18% (6–18%) (these are taken to be uncorrelated among the backgrounds); (k) higher order correction for the V +jets cross section, 20% (20%); (l) V +heavy flavor jet cross section correction, 30% (30%); and (m) multijet background, 82–100% (uncorrelated $\tau\nu$ and $\tau\tau$).

The upper limits on the Higgs boson cross section are obtained using the modified frequentist method [20]. For the $\tau\nu$ analysis, the test statistic is the negative log likelihood ratio (LLR) derived from the M_{jj} distribution. For the $\tau\tau$ analysis, the LLR is formed from the $NN_{Z_{\text{jets}}}$ final neural network variable. The confidence levels CL_{s+b} (CL_b) give the probability that the LLR value from a set of simulated pseudo-experiments under the signal plus background (background-only) hypothesis is less likely than that observed, at the quoted C.L. The hypothesized signal cross sections are scaled up from their SM values until the value of $CL_s = CL_{s+b}/CL_b$ reaches 0.05 to obtain the limit cross sections at the 95% C.L., both for expected and observed limits. In the calculation, all contributions to the systematic uncertainty are varied, subject to the constraints given by their estimated values, to give the best fit [21]. The correlations of each systematic uncertainty among signal and/or background processes are accounted for in the minimization.

The ratios of the expected and observed upper limits to the SM expectations are shown in Table II for the two channels separately and combined. For all Higgs masses, the observed limits are within 1σ of the expected limits. At $M_H = 115$ GeV, the observed (expected) 95% C.L. limit is 29 (28) times that predicted in the SM for the seven signal processes considered

TABLE II: Expected and observed 95% C.L. upper limits on the Higgs boson production cross section relative to the SM predicted value, for the $\tau\nu$ and $\tau\tau$ analyses separately and combined.

M_H (GeV)	$\tau\nu$ analysis		$\tau\tau$ analysis		Combined	
	exp.	obs.	exp.	obs.	exp.	obs.
105	33	27	39	36	24	20
115	42	35	43	47	28	29
125	62	60	60	65	40	44
135	105	106	87	61	63	50
145	226	211	158	95	120	82

in the combined $\tau\nu$ and $\tau\tau$ analyses. This is the first limit on SM Higgs production using final states involving hadronically decaying tau leptons. These results contribute to the sensitivity of the combined Tevatron search for low mass Higgs bosons [2].

We thank the staffs at Fermilab and collaborating institutions, and acknowledge support from the DOE and NSF (USA); CEA and CNRS/IN2P3 (France); FASI, Rosatom and RFBR (Russia); CNPq, FAPERJ, FAPESP and FUNDUNESP (Brazil); DAE and DST (India); Colciencias (Colombia); CONACyT (Mexico); KRF and KOSEF (Korea); CONICET and UBACyT (Argentina); FOM (The Netherlands); STFC and the Royal Society (United Kingdom); MSMT and GACR (Czech Republic); CRC Program, CFI, NSERC and West-Grid Project (Canada); BMBF and DFG (Germany); SFI (Ireland); The Swedish Research Council (Sweden); CAS and CNSF (China); and the Alexander von Humboldt Foundation (Germany).

[a] Visitor from Augustana College, Sioux Falls, SD, USA.

[b] Visitor from Rutgers University, Piscataway, NJ, USA.

[c] Visitor from The University of Liverpool, Liverpool, UK.

[d] Visitor from Centro de Investigacion en Computacion - IPN, Mexico City, Mexico.

[e] Visitor from ECFM, Universidad Autonoma de Sinaloa, Culiacán, Mexico.

- [f] Visitor from Helsinki Institute of Physics, Helsinki, Finland.
 - [g] Visitor from Universität Bern, Bern, Switzerland.
 - [h] Visitor from Universität Zürich, Zürich, Switzerland.
 - [‡] Deceased.
- [1] M. Carena, J.S. Conway, H.E. Haber and J.D. Hobbs, arXiv:hep-ph/0010338.
 - [2] For references to the full set of Higgs searches by the CDF and D0 collaborations, see arXiv:hep-ex/0903.4001 (2009).
 - [3] S. Abachi *et al.* (D0 Collaboration), Nucl. Instrum. Methods Phys. Res. A **338**, 185 (1994); V.M. Abazov *et al.* (D0 Collaboration), Nucl. Instrum. Methods Phys. Res. A **565**, 463 (2006); V.M. Abazov *et al.*, Nucl. Instrum. Methods Phys. Res. A **552**, 372 (2005).
 - [4] V.M. Abazov *et al.* (D0 Collaboration), Phys. Rev Lett. **101**, 241802 (2008).
 - [5] V.M. Abazov *et al.* (D0 Collaboration), Phys. Rev D **71**, 072004 (2005); erratum *ibid* **77**, 039901 (2008).
 - [6] G.C. Blazey *et al.*, FERMILAB-PUB-00-297 (2000).
 - [7] M.L. Mangano *et al.*, J. High Energy Phys. 0307, 001 (2003); we use ALPGEN version 2.05.
 - [8] T. Sjöstrand *et al.*, arXiv:hep-ph/030815 (2003); we use PYTHIA version 6.319.
 - [9] E. Boos *et al.*, Phys. Atom. Nucl. **69**, 1317 (2006); E. Boos *et al.* (CompHEP Collaboration), Nucl. Instrum. Methods Phys. Res. A **534**, 250 (2004).
 - [10] J. Pumplin *et al.*, J. High Energy Phys. 0207, 012 (2002).
 - [11] The V +jets cross sections are normalized using MCFM version 3.45 by J. Campbell and R.K. Ellis, Phys. Rev. D **65**, 113007 (2002). The higher order $t\bar{t}$ cross section is taken from N. Kidonakis and R. Vogt, Phys. Rev. D **68**, 114014 (2003).
 - [12] T. Hahn *et al.*, arXiv:hep-ph/0607308 (2006).
 - [13] A. Djouadi, J. Kalinowski, and M. Spira, Comp. Phys. Commun. **108**, 56 (1998).
 - [14] S. Jadach *et al.*, Comp. Phys. Commun. **76**, 361 (1993).
 - [15] In events with true \cancel{E}_T due to non-interacting particles, \cancel{E}_T and \cancel{T}_T tend to be aligned, whereas for events with mismeasured jets in the calorimeter they do not.
 - [16] T. Scanlon, FERMILAB-THESIS-2006-43 (2006).
 - [17] V. Barger, J. Ohnemus, and R.J.N. Phillips, Phys. Rev D **48**, 3953 (1993).
 - [18] T. Andeen *et al.*, FERMILAB-TM-2365 (2007).

- [19] V.M. Abazov *et al.* (D0 Collaboration), Phys. Rev. Lett. **101**, 062001 (2008).
- [20] A. Read, J. Phys. G: Nucl. Part. Phys. **28**, 2693 (2002); T. Junk, Nucl. Instrum. Methods A **434**, 435 (1999).
- [21] W. Fisher, FERMILAB-TM-2386-E (2006).